
Universiteit
Leiden
The Netherlands

From electrons to stars : modelling and mitigation of radiation damage effects on astronomical CCDs

Prod'homme, T.

Citation
Prod'homme, T. (2011, November 22). *From electrons to stars : modelling and mitigation of radiation damage effects on astronomical CCDs*. Retrieved from https://hdl.handle.net/1887/18136

Version:	Corrected Publisher's Version
License:	Licence agreement concerning inclusion of doctoral thesis in the Institutional Repository of the University of Leiden
Downloaded from:	https://hdl.handle.net/1887/18136

Note: To cite this publication please use the final published version (if applicable).

Chapter 5

Stress-testing a fast analytical Charge Transfer Inefficiency model

ESA's Gaia mission aims to create a complete and highly accurate stereoscopic map of the Milky Way. The stellar parallaxes will be determined at the micro-arcsecond level, as a consequence the measurement of the stellar image location on the CCD must be highly accurate. During the mission solar wind protons will create charge traps in the CCDs of Gaia, thus drastically increasing the CCD Charge Transfer Inefficiency (CTI). CTI will distort the stellar images and induce a significant charge loss for all the Gaia measurements. If not properly mitigated, the CTI effects introduce a strong systematic bias in the image location estimation and cause a significant degradation of its precision. The Gaia Data Processing and Analysis Consortium chose to mitigate the CTI effects by an iterative forward modelling approach that requires the accurate modelling of the stellar image distortion and charge loss for each observation. In this scheme, the final astrometric accuracy of Gaia directly depends on the capability of a fast analytical model of CTI effects, a so-called Charge Distortion Model (CDM), to reproduce the image distortion. In this chapter we assess the capability of a fast analytical Charge Distortion Model, proposed by Short et al. (2010), to reproduce experimental data. We developed a rigorous procedure that compares at the sub-pixel level the model outcomes to images affected by CTI extracted from experimental tests. We show that the tested CDM candidate has the capability to accurately reproduce the test data acquired on a highly irradiated device operated in Time-Delayed Integration (TDI) mode for a wide range of signal levels and different CCD illumination histories. In particular we are able to demonstrate that the level of agreement obtained is enough to recover the CTI-induced image location bias by at least a factor ten, and thus enables the potential recovery of the required final astrometric accuracy. The calibration of such a model is however a complicated enterprise and potentially problematic. By comparing the performance of the model in different conditions of use, we discuss different calibration schemes and give recommendations for necessary improvements of this model that will ease the calibration process. The mitigation of CTI effects using a forward modelling approach, as done for Gaia, is also interesting for other space missions, in particular future ESA missions currently under consideration, Euclid and Plato.

T. Prod'homme, M. Weiler, S.W. Brown, A.D.T. Short, A.G.A. Brown, B. Holl
In preparation

5.1 Introduction

Gaia is a European Space Agency mission that aims to create the most complete and accurate stereoscopic map to date of the Milky Way by collecting parallaxes, proper motions, radial velocities, and astrophysical parameters for about one billion stars, one percent of the estimated stellar population in our galaxy (Perryman et al. 2001; Lindegren et al. 2008). Gaia, to be launched in 2013, will orbit around the second Lagrange point (L2) and constantly spin around its own axis such that its two telescopes scan a great circle on the sky several times a day. Due to the satellite spinning motion, the star images will not remain stationary during an observation but will transit across the focal plane. The stellar transits are recorded in a single focal plane covered by 106 CCDs. To integrate the stellar flux along the transits, the CCDs are operated in Time-Delayed Integration (TDI) mode. In this mode a CCD is constantly read out and the charge transfer rate is synchronized with the motion of the stellar images over the focal plane.

In order to reconstruct the astrometric motion on the sky for a particular star and estimate its astrometric parameters, the different times of observation must be determined very accurately. If the attitude of the satellite is known, determining a time of observation effectively corresponds to determining the stellar image location on each CCD before readout (Lindegren & Bastian 2011; Bastian & Biermann 2005). The anticipated Gaia astrometric accuracy is extreme and sets a stringent requirement on the estimation of the stellar image location per CCD star transit (see Chapters 3 and 4, and de Bruijne 2005). For instance the end-of-mission statistical parallax standard error is required to be 26 micro-arcseconds for a G2V star of magnitude 15, which corresponds to an uncertainty on the location of stellar images on the CCD of 0.0045 pixels (~ 0.27 milli-arcseconds) for a single transit.

The displacement of atoms in the silicon lattice of the Gaia CCDs by solar flare protons will result in the creation of energy levels in the semiconductor band gap. These energy levels trap the signal carriers (electrons in a n-type device) and consequently increase the CCD Charge Transfer Inefficiency (CTI). The stochastic capture and release by the traps of the charges result in a significant charge loss and distortion of the stellar images. Experimental tests conducted on Gaia irradiated CCDs (e.g., Hopkinson et al. 2005; Pasquier 2011) as well as in depth simulation-based studies (Chapters 3 and 4) have demonstrated that CTI effects will significantly affect the determination of the stellar image location and thus the final astrometric accuracy of Gaia, if not properly taken into account in both the Gaia data processing and the CCD design and operation. Indeed the charge loss induces an irreversible loss of accuracy (of the order of a few percent) that is independent of any image location estimator and can only be avoided by the use of hardware CTI countermeasures that physically prevent the trapping, such as periodical Charge Injections (CI). The stellar image distortion due to CTI introduces a bias in the image location determination, which can be as large as 0.2 pixels for a magnitude 15 star. This number should be compared to 0.0045 pixels, the required image location accuracy mentioned above. This important sensitivity of Gaia to CTI can be imputed to a number of factors (see Chapters 1 and 2), among which: a harsh radiation environment, a low level of shielding resulting from stringent weight constraints,

special CCD operating conditions (see Section 5.3), and a demanding measurement accuracy.

Hardware CTI countermeasures (Section 5.3) can only prevent a part of the trapping, and as a consequence CTI must be taken into account in the Gaia data processing. Correcting for CTI is a complicated task; CTI effects are stochastic, they depend non-linearly on the stellar brightness, and they are non-repeatable for a particular star or magnitude as they depend on the CCD illumination history prior to the stellar transit of interest. Besides it has to be noted that the calibration of any software-based procedure will be further complicated, first, by the lack of CTI-free measurements: as the Gaia launch date is close to the solar maximum activity, even the very first measurements will be affected by CTI to some degree. Secondly, by the lack of information regarding the CCD illumination history and the stellar observations themselves: due to a limited telemetry rate the Gaia observations will consist of truncated one-dimensional charge profiles of 6 to 12 pixels in the stellar transit direction (see Section 5.3).

For these reasons conventional CTI correction procedures cannot be applied and the Gaia Data Processing and Analysis Consortium (DPAC) has developed a novel CTI mitigation procedure that relies on the forward modelling of each observation including the radiation damage effects. In this scheme, the true image location and flux are estimated by comparing the actual observation to a predicted charge profile, for which the CTI-induced distortion is modelled by an analytical model of the CTI effects, a so-called Charge Distortion Model (CDM). This enables the mitigation for any kind of source including complex ones (such as binaries, triple stars, extended or resolved objects) and does not affect the noise properties of the observations by avoiding a direct correction of the raw data. In Chapter 3 we demonstrated that this approach allows for a precise and bias-free estimation of the true image location from an observation affected by CTI effects (referred to as damaged observations). The efficiency of such a scheme, and consequently the final Gaia astrometric accuracy, relies on the capability of a CDM to accurately reproduce the damaged observations. The distortion will have to be computed for each CCD observation (~ 700 over the full mission duration) of each star (~ 1 billion). Moreover the image, the Line Spread Function (LSF, the one-dimentional Point Spread Function), and the CDM parameters are obtained from the same data, thus necessitating an iterative procedure (i.e. repeated several times for each observation). Hence the CDM must at the same time realistically reproduce the radiation damage yet remain simple enough to be computationally inexpensive for use in the Gaia data processing pipeline.

The model presented by Short et al. (2010) constitutes the current best CDM candidate. Chapter 3 showed that this model is capable of reproducing simulated damaged observations accurately enough so that most of the CTI-induced bias in both the image location and flux estimation can be removed. For this purpose the damaged observations were simulated by a detailed and physical Monte Carlo model of CTI effects that simulates the transfer of charges at the CCD pixel electrode level (Chapter 2). The calibration of the model parameters was performed for each stellar magnitude and for a unique illumination history making use of the true instrument LSF and a high number

of observations. This chapter[1] goes one step further and assesses the model capability to reproduce *experimental data* under realistic calibration conditions and for a wide range of signal levels and different illumination histories. Making use of the results from Chapter 3 we are able to evaluate if the overall agreement between model predictions and experimental data reaches the requirements set by the Gaia astrometric accuracy. After a presentation of the CDM candidate (Section 5.2) and the description of the Gaia CCD design and operation (Section 5.3), we give an overview of the experimental data used for the purpose of this comparison exercise (Section 5.4). Section 5.5 provides a description of our comparison procedure and in particular how the CDM parameters can be calibrated to fit the damaged experimental data at the sub-pixel level. In Section 5.6, we present the highest level of agreement with the experimental data achievable by CDM and compare it to agreements obtained for a set of more realistic CDM parameter calibration schemes. Finally, in Section 5.7, we discuss the limits and performance of the tested CDM candidate in the context of the Gaia CTI mitigation procedure, and give recommendations regarding the use of CDM and its further improvement.

5.2 Charge Distortion Model

The current best CDM candidate for implementation in the Gaia data processing is the physically motivated fast analytical CTI effects model presented by Short et al. (2010), hereafter we directly refer to it as CDM. To cope with the computational speed requirement CDM suppresses the treatment of the numerous charge transfer steps required to transfer and build the signal from one end of the CCD to the other, and computes the signal transit in a single calculation. This implies several important simplifications, the most relevant for this chapter are detailed in the following (for a complete explanation see Short et al. 2010).

5.2.1 Principles

Statistical treatment of the trapping processes

The model is based on the common Shockley-Read-Hall formalism (Shockley & Read 1952; Hall 1952), which describes the capture and release of a charge by an individual trap as a decay process with an associated characteristic time constant. The Charge Distortion model does not compute the capture and release probabilities for individual traps. Instead the capture and release of electrons is treated statistically by integrating over the total amount of traps present in the CCD. It thus implicitly considers a homogeneous distribution of the traps within a particular geometrical confinement volume V. The latter corresponds to the volume occupied by an electron packet at Full Well Capacity (FWC).

Trap species

As a result of the displacement of silicon atoms in the CCD silicon lattice (caused by radiation damage), interstitial atom-vacancy pairs are created. These vacancies diffuse

1. The first results of this study were presented at the 2010 SPIE conference in San Diego (Prod'homme et al. 2010), this work now supersedes in methodology and scope the former results.

and bind with other vacancies or impurities (e.g., oxygen, carbon, phosphorus atoms) present in the lattice. A vacancy-impurity complex is usually referred to as a trap species as the energy level and capture cross-section σ vary from one type of complex to the other. In CDM an arbitrary number of trap species J can be used, and a set of three parameters is associated with each trap species: σ_j, τ_j the release time constant, and ρ_j the trap density. In principle the release time constant, τ, varies as a function of the trap energy level, the temperature T, and σ_j (see e.g., Chapter 2). However in CDM this parameter is directly set and thus independent from the temperature and the capture cross-section. As a consequence the trap species resulting from a fit of the CDM predictions to a particular dataset may not correspond to a real vacancy-impurity complex.

Constant electron density distribution within a growing signal confinement volume
The total number electrons trapped depends on the capture time constant τ_c. τ_c depends on the temperature T, the trap capture cross-section σ, and the electron density distribution n_e. In CDM, for a particular number of electrons N_e in a pixel, the density distribution is assumed to be constant within the charge cloud volume V_c:

$$n_e = N_\mathrm{e}/V_\mathrm{c} \tag{5.1}$$

The parameter β determines the growth of V_c as a function of signal level:

$$V_\mathrm{c} = V\left(\frac{N_\mathrm{e}}{\mathrm{FWC}}\right)^{\beta} \tag{5.2}$$

Despite the complexity of the Gaia pixel architecture (cf. Section 5.3), CDM considers only one parameter β for the entire range of signal levels: from 0 $\mathrm{e}^-$to FWC ($\sim$ 190 000 e^-). As we shall see in Section 5.6.3, this constitutes one of the main limitations of CDM when one aims to reproduce with a single set of parameters a set of stellar images including different magnitudes.

Illumination history
The CTI induced distortion and charge loss for a particular stellar image depends on the state of each encountered trap prior to the stellar transit of interest. The state of these traps is set by the CCD illumination history. As traps are not modelled individually in CDM but treated in a statistical way, for a particular illumination history CDM computes the total fraction of filled traps, the trap occupancy level. The effect on the trap occupancy level of both a discrete event (e.g., CI) and a continuous illumination (background light, S_DOB) can be taken into account. Depending on the use of CDM in image mode or TDI mode, the treatment of the illumination history involves different assumptions. In the following section along with the description of our specific use of CDM, we detail the associated assumptions.

5.2.2 Usage

In this chapter we assess the performance of CDM using its TDI mode only. This is mainly due to the fact that the experimental test data (Section 5.4) we aim to reproduce

Parameter	Description	Fixed value or [interval]
	CCD parameters	
T	temperature	163 K
V	geometrical confinement volume	24 μm $\times$ 11 μm $\times$ 0.75 μm
FWC	CCD full well capacity	190 000 e^-
P_{TDI}	TDI period	0.9828 ms
N_T	number of pixel transfers	4500
β	electron cloud growth parameter	$[10^{-5}$ - 1]
	Trap parameters	
J	number of trap species	[1 - 7]
ρ_j	number of traps per pixel	$[10^{-5}$ - $10^{2}]$
σ_j	capture cross-section	$[10^{-26}$ - $10^{18}]$ m^2
τ_j	release time constant	$[10^{-4}$ - $10^{2}]$ s
	Experiment parameters	
t_{CI}	time since last charge injection	$[3.0\,10^{-3}$ - $1.2\,10^{2}]$ s
S_{DOB}	diffuse optical background	[0 - 240] e^-sample^{-1} s$^{-1\star}$

Table 5.1 — This table presents the parameters necessary to perform a CDM simulation. We indicate the used value for the fixed parameters. And we present, for the free parameters, the interval over which they are allowed to vary during the calibration procedure.
*A sample corresponds to one pixel for a two-dimensional simulation and 12 pixels for a one-dimensional simulation.

with CDM were acquired with a CCD operated in TDI mode (to reproduce the in-flight Gaia operating conditions). However it is important to note that, although the Gaia CCDs will be operated in TDI mode, the imaging mode of CDM may also be used in the Gaia data processing: first, to model the effects induced by CTI in the serial register, and, second, to initialize in the most realistic way possible the trap occupancy level given a time since last CI. For this particular study the serial CTI can be neglected (see section 5.4.1). And, in order to compute the initial trap occupancy given a time since last CI, we assumed that all the traps are filled by a CI (Eq. (34) in Short et al. 2010). The validity of such an assumption is discussed in Section 5.7.2.
All the parameters of a CDM simulation are detailed in Table 5.1. During the whole comparison the parameters always kept fixed are: T, V, FWC, P_{TDI} the TDI period (i.e. pixel transfer period in the CCD image area), and N_T the total number of transfers in the image area. The fixed values are indicated along with the parameters in Table 5.1. From the test data we also set t_{CI} the time since last CI corresponding to each specific test (cf. Section 5.4). In principle the background light S_{DOB} could also be estimated from the RC data itself and set to a fixed value however we chose to let this parameter free as its estimation is not entirely reliable. The free, i.e. calibrated, parameters are thus the trap parameters for each trap species j: ρ_j, σ_j and τ_j, along with the background light S_{DOB}, and the electron cloud growth parameter β. The number of trap species J to be included in a CDM simulation is an important issue for the Gaia data processing. As we shall see in Section 5.6 the optimal number of trap species to be considered depends on the calibration scheme.
During the mission the Gaia CCDs will acquire two-dimensional stellar images, but

only one-dimensional binned images will be sent to ground (see Section 5.3). The question of using CDM to perform a 1D or a 2D forward modelling of the Gaia observations in the image parameter estimation and CTI mitigation procedures is thus a key issue. It is a problematic question in terms of calibration and instrument modelling, because the two-dimensional information about the instrument PSF will be very limited, only the brightest stars will not be binned. The use of relatively poorly characterized PSFs might introduce undesired effects in the sensitive and critical image location estimation. And it is also problematic in terms of computational power and time requirements, since the use of CDM to distort a 12 by 12 pixels CTI-free input signal requires 12 times the computational load of the same computation for 1 by 12 pixels signal. In the following we will thus asses the capability of CDM to reproduce experimental test data using it in 1D or 2D.

5.3 Gaia CCD design and operation

The Gaia CCDs (see Short et al. 2005) are back-illuminated and full frame devices. They are custom made by e2v technologies and referenced as CCD91-72. The CCD image area contains 4500×1966 pixels (parallel $\times$ serial). Among the 4500 pixel rows only 4494 are light-sensitive: six rows are blocked by an aluminum shield. Each pixel contains a supplementary buried channel (SBC, or notch) and an anti-blooming drain. The SBC corresponds to a particular doping implant that confines to a smaller volume (than the buried channel) small charge packets so that these small packets encounter less traps. As shown by Hopkinson et al. (2005) and as confirmed in Chapter 2, in Gaia CCDs, the SBC-induced CTI mitigation stops to be effective for charge packets greater than ~ 3000 e^-. Due to the spinning motion of the satellite and the operation of the CCD in TDI mode, it is important to realize that most of the Gaia measurements will be faint when the signal starts to be integrated (i.e. at the beginning of the star transit across the CCD). In fact, for more than half of their CCD transit, the entire image of stars fainter than magnitude [2] $G = 16$ are transferred in the SBC only. As a consequence, bright and faint stars will experience different levels of trapping. And the CTI effects cannot in principle be modelled across a wide range of signal levels without an explicit modelling of the SBC.

The Gaia CCDs allow the periodical injection of electrons. Along with the SBC, CIs constitute one of the main hardware CTI countermeasures to be used by Gaia. A CI consists of the injection of a certain number of electrically generated charges in the first CCD pixel row. The CI is then transfered through the CCD image area so that vacant traps throughout the CCD can be filled. A direct consequence is that stellar images transiting right after a CI experience less damage. The CIs also have the advantage of dominating and thus reseting the illumination history. This eases the process of understanding the CTI effects independently from the CCD illumination history. The traps with characteristic release time constants greater than the CI period are permanently filled by the artificially generated charges. However traps with shorter release time

2. The Gaia G-band magnitude is a broad-band, white-light magnitude in the wavelength range 300 – 1000 nm defined by the telescope transmission and CCD quantum efficiency. $G = V$ for an un-reddened A0V star (Jordi et al. 2010; Perryman et al. 2001).

constants remain active because they have the time to release their charges before the next CI. The expected CI period to be used on-board Gaia is 1 s.
As already mentioned, the Gaia CCDs will be operated in TDI mode to integrate the light along the star transits. Star transits will always be parallel to the CCD parallel transfer direction [3]. In the following we thus refer to it as the 'along-scan' direction or AL. Accordingly the CCD serial direction is referred to as the 'across-scan' direction, AC. Gaia will continuously produce a large amount of data on-board thanks to its 106 CCDs, but due to its limited telemetry capacity only a part of it will be downlinked. The transmitted data for each star corresponds to a window of pixels centered on the pixel containing the maximum flux. The AL width of a telemetry window will vary as a function of the star magnitude: 12 AL pixels for stars brighter than magnitude 16 and 6 AL pixels for the fainter stars. Also for most of the stars the telemetry window will be binned across-scan. As a result, only one-dimensional data will be available for these stars.

5.4 Experimental tests

To characterize and evaluate the impact of the CTI effects on the Gaia measurements and to test and optimize the different potential hardware CTI countermeasures, the industrial partners in the Gaia project performed several campaigns of laboratory experiments on irradiated CCDs with an architecture and parameters as anticipated for the Gaia flight CCDs. The prime contractor for Gaia, EADS Astrium, conducted up to now four of these test campaigns, from hereon referred to as Radiation Campaigns (RC). For these four RCs, Astrium used a test setup (Pasquier 2011) which closely reproduces the in-flight conditions and simulates the transit of stars over an irradiated Gaia CCD. In the following we give a brief description of the test setup. Then we present the subset of data we used in our comparison, which is extracted exclusively from Astrium's second RC (from hereon referred to as RC2). Finally we explain how the data acquired in the non-irradiated part of the tested CCD is used to build a CTI-free signal which serves as input to the CDM.

5.4.1 Experimental test setup

All the tests performed by Astrium were carried out on irradiated Gaia CCDs. The tested devices include an irradiated region with a radiation dose of 4×10^9 protons cm^{-2} (10 MeV equivalent), a non-irradiated region, and a transition region between them. The non-irradiated region is the closest to the readout node. In the irradiated region the serial register was also irradiated, but one can to first order ignore the effects of the radiation induced serial CTI. The stellar image located the furthest from the readout node will effectively undergo only a few hundreds of serial transfers in the irradiated region (to be compared to 4500 parallel transfers). The AC size of the window is large enough to contain the majority of the redistributed electrons, so that charge loss due to serial CTI can be ignored. Serial CTI distorts the shape of the AC profile, however this distortion cannot be observed due to the AC binning. For these reasons we chose to ignore the effect of serial CTI in this study.

3. The maximum deviation in the serial direction is expected to be of the order of 4 pixels at readout

The CCD was operated at different temperatures including the Gaia operating temperature of $163\,\mathrm{K}$. To produce point-like sources playing the role of artificial stars, a mask with punched holes was used. The artificial stellar brightness was determined by the illuminating source (LED) brightness. The mask was translatable to reproduce the star motion and to operate the CCD in TDI mode. Due to the continuous readout and the faint luminosity of the sky background, the background light in Gaia CCDs is expected to remain very low over the mission independent of the line of sight. As a consequence, particular care was taken to introduce as little background light as possible. To recreate in-flight conditions the stellar images were binned in the AC direction.

5.4.2 The test dataset

RC2 (see Pasquier 2011; Georges 2008; Brown 2009b) focused on the evaluation and characterization of repeated artificial charge injections as a potential CTI hardware countermeasure. The CI parameters are the level, duration and period. The CI level is the number of electrons injected in one pixel. The duration corresponds to the number of subsequent CCD pixel rows in which the charges are injected. Finally the period is the time separating two consecutive CIs. RC2 data proved to be particularly suitable for our comparison as each of the parameters was carefully investigated which provided us with a set of well defined and understood tests carried out at different temperatures, CI levels, durations, and delays between the charge injection and the first 'star' crossing the CCD.
To compare the CDM predictions and the experimental data we focus on a subset of the RC2 data at the operational temperature of Gaia for which the CI level and duration were kept fixed. The delay between the CI and the first star transit was varied as well as the level of illumination, or artificial star magnitude. This allows us to evaluate how well the CDM can reproduce with a single set of parameters a damaged star image or a set of images for different illumination levels ($13.3 < G < 20$) and for different time domains. The CI delays range from 30 ms to 120 s. Multiple scans were performed in each test and, as a result, for a single set of experimental parameters (temperature, star brightness, CI delay) we can extract an over-sampled damaged profile to compare with the CDM outcomes.

5.4.3 Modelling the CDM input signal

The accumulated data in the non-irradiated part of the CCD are used to create a reference curve. This curve is representative of the CCD illumination conditions and is used as input for the simulations with CDM. With only one dimensional stellar images available, the reference curves are actually LSFs (Line Spread Function, the PSF integrated in the across-scan direction), which are subsequently modelled using spline functions [4]. As already mentioned we want to investigate the performance of CDM in 1D and 2D. To generate a two-dimensional input signal for our simulations we use the original reference curve and assume that the AL and AC profiles are the same: $P(x, y) = L(x) \times L(y)$, where L is the undamaged reference curve and P the result-

4. The spline functions are characterised by the positions of a set of knots along the LSF profile and the parameters that describe the set of polynomials linked by the knots.

ing CDM input image. This process allows us to recover to some extent the original properties of the illumination set-up. For both one-dimensional and two-dimensional input, the integrated flux of the reference curve is scaled to produce a CDM input image for each artificial star magnitude.

5.5 Model-data comparison methodology

5.5.1 Comparison procedure

In this section we present the procedure we used for all the comparisons between the RC2 test data and the CDM outcomes. First a target charge profile and a corresponding undamaged reference curve are defined. The target charge profile is the experimental data including CTI effects that the CDM eventually aims to reproduce. Thanks to the damaged profile over-sampling, the comparison between the model and the data is better constrained and the derived parameters are independent of the sub-pixel position of the image profile. To perform a direct comparison between the experimental data points and the charge profile simulation with CDM, the sampling scheme specific to each of the target charge profiles is extracted. This sampling scheme is then applied to the PSF generated from the reference curve, in order to create the CDM image inputs. In this way the required number of CDM instances to generate an n times over-sampled simulated profile is n. Each of the n CDM instances is calculated with a single predefined set of parameters. Once the instances are completed, the individual CDM predictions are binned in the AC direction and each data point is then placed at the correct sub-pixel position according to the original sampling scheme so as to form an over-sampled predicted damaged profile. The actual comparison, i.e. the computation of the agreement (cf. Section 5.5.2), is performed using the over-sampled CDM prediction and target damaged profile.

5.5.2 Determination of the best-fitting CDM parameters

Our calibration procedure consists of finding a set of CDM parameters that optimizes the agreement between the CDM outcomes and a set of pre-selected data. The agreement between a predicted and an individual target over-sampled charge profile is quantified via the computation of a comparison criterion or goodness-of-fit parameter g. The latter is an altered version of the usual χ^2 and is defined as follows:

$$g = \frac{1}{S}\frac{1}{F}\sum_{i=0}^{S-1}\frac{\left(\lambda\left(k_i\right) - N\left(k_i\right)\right)^2}{\sigma_i^2} = \frac{\chi^2}{S\,F} \tag{5.3}$$

where λ is the simulated damaged charge profile, N the RC2 target charge profile, k_i a particular sub-pixel position, σ_i the noise, S the total number of data points, and F the total integrated flux. The noise is considered to be the quadratic sum of the photon-noise and the readout noise. The photon-noise is assumed to follow Poisson statistics with a standard deviation of $\sqrt{N}$ and r is assumed to have the constant value of 4.35 e^-(the typical measured value for the Gaia CCDs):

$$\sigma_i^2 = N\left(x_i\right) + r^2 \tag{5.4}$$

Depending on the chosen calibration scheme, one can attempt to fit with a single set of CDM parameters a variety of target profiles. But due to the fact that CDM does not provide a perfect representation of the CTI effects, we use two scaling factors, S and F, in our comparison criterion: S is required when one attempts to simultaneously fit different target charge profiles with different numbers of data points per pixel, and F to simultaneously fit charge profiles of different magnitudes. If these scaling factors are not present, the fit is biased towards the brightest magnitude and the most over-sampled profiles.
The calibration procedure involves two different optimization algorithms. In a first instance, we probe the entire parameter space (within the specified intervals in Table 5.1) by using an evolutionary algorithm [5] that includes two mechanisms: mutation and cross-over. It is applied on an initial population of 1 million parameter sets and evolves towards smaller g, generation after generation. Generally for such a large initial population, the best agreement does not change significantly after 10 generations. In a second step, the set of parameters found is further improved by using the downhill simplex minimization method (Nelder & Mead 1965). Due to the large number of parameter sets tested, this procedure ensures that the resulting parameter set does not correspond to a local minimum.

5.5.3 Calibration schemes

During the Gaia mission a number of parameters are expected to remain constant or vary only slightly for a particular CCD. These parameters are the number of trap species as well as the characteristic capture cross-section and release time constant for each trap species. These two last parameters are temperature dependent, however the temperature variation accross a single CCD is negligible. The trap density will vary as a function of the solar activity but if one considers short time scales (from several hours to a couple of days), this parameter can be assumed to remain constant. In principle, a CDM sufficiently accurate for describing the CTI effects at any signal level and for any kind of illumination history could be used with a single set of parameters for all the observations coming from one particular CCD, and thus the CDM parameters could be calibrated on a per CCD basis or at least on per CCD stitch block [6] basis. However as mentioned in Section 5.2, CDM uses a number of simplifications regarding in particular the modelling of the electron density distribution. For this particular reason, a calibration of the CDM parameters over a smaller set of observations selected on a per magnitude or a per illumination history basis is expected to give better results and should in principle remain practical for the Gaia data processing.
In Section 5.6 we present the resulting agreement between the CDM outcomes and the experimental data for four different calibration schemes of the CDM parameters; the CDM parameters are optimized to fit:

5. `http://watchmaker.uncommons.org/`

6. CCDs are manufactured using photo-lithographic masks. Due to practical manufacturing constraints, the masks are smaller than the image area of large format devices like the Gaia CCDs. As a result, a large format CCD consists in the assemblage of smaller 'CCD units' with slightly different parameters called stitch blocks.

1. a single target charge profile. This would correspond to a calibration of the CDM parameters for each observation of a particular star obtained under very similar conditions. Although impractical in the context of the Gaia data processing, this allows the assessment of the best agreement obtainable for this particular CDM candidate.
2. a set of target charge profiles with the same signal level but different CI delays. This corresponds to a calibration of the CDM parameters on a per stellar magnitude basis.
3. a set of target charge profiles with the same CI delay but different signal levels. This corresponds to a calibration of the CDM parameters on per CI delay basis.
4. the entire dataset including different signal levels and CI delays. This corresponds to a calibration of the CDM parameters on a per CCD basis.

Note that due to the nature of the experimental data, the disturbing effect of a star located in between the star of interest and the last CI cannot be accounted for in any of these calibration schemes. Chapter 4 showed that the effect of disturbing stars on the CTI calibration at the image processing stage is only significant for bright stars. This effect may be further investigated by, for instance, repeating the procedures described in this chapter on the 'sky-like' data acquired during RC3 and RC4 for which a mask with a pseudo-realistic sky-pattern was used.
In order to compare the agreements resulting from different calibration schemes at the level of individual predicted and target profiles, we make use of the reduced χ^2, χ^2_r:

$$\chi^2_r = \frac{\chi^2}{S - (3\,J + 2)} \tag{5.5}$$

where $3\,J + 2$ is the number of free parameters. χ^2_r is not used in the optimization of the CDM parameters, but only for the purpose of a final comparison between different calibration schemes.

5.6 Results

In the following we present the results of our comparison between the RC2 test data and the CDM predictions obtained using different calibration schemes. By establishing the performance of the tested CDM candidate, we are also able to identify some of its current limitations. Moreover we address for each calibration scheme two key issues for the Gaia data processing by characterizing the impact on the final agreement reached by the tested CDM candidate of: (i) the number of trap species included in a CDM simulation, and (ii) performing one-dimensional or two-dimensional CDM simulations.

5.6.1 The best agreement achievable

In this first step of our comparison, CDM is employed to reproduce each individual one-dimensional damaged profile from RC2; we thus proceed to an independent calibration of the CDM parameters for each available signal level and distance to the

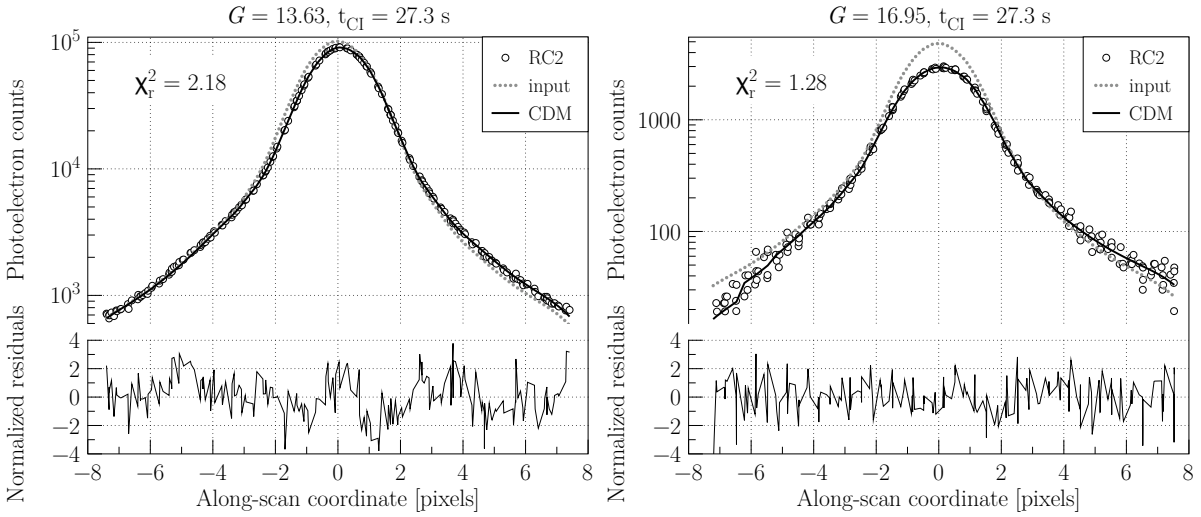

Figure 5.1 — Comparison between the RC2 test data (black circles) and the CDM predictions (black continuous lines) for a unique CI delay ($\sim$ 27 s) and two different signal levels: $G = 13.63$ (left) and $G =$16.95 (right). The grey dotted line represents the model input signal. While the top part of the figure allows for a direct and qualitative comparison between test data and CDM predictions, the bottom part shows the normalized residuals i.e. the difference between actual and predicted profiles divided by the photon noise. To quantify the agreement between model and data we also indicate the values of χ^2_r. The CDM prediction corresponds to the best fit to the shown RC2 charge profile. The best-fitting model parameters are presented in Table 5.2. The charge transfer in the CCD image area is from right to left (i.e. the leftmost samples are the first to be read out). The same convention is applied for all the figures representing charge profiles.

preceding CI (or time since last CI). In these conditions the best level of agreement between the CDM predictions and the test data can be obtained. Hence, in this way, we can assess the ultimate performance of the tested CDM candidate.

CDM can always achieve a very good fit to any specific damaged charge profile. Fig. 5.1 is an illustration of this capability to reproduce a particular damaged profile for two different signal levels (note that the ordinate scale is logarithmic). As illustrated in the bottom part of Fig. 5.1, no significant systematic variation of the normalized residuals can be observed across the profile, this means that the same level of agreement is achieved over the entire profile: peak, leading and trailing edges.

For these calibration conditions we were able to evaluate the number of trap species required to achieve the best agreement possible and wether the simulations must be performed in one dimension (1D) or two (2D). It is essential to address these two questions for the Gaia data processing and also in order to understand what level of realism is achieved by the tested CDM candidate. For each signal level and CI delay, the calibration procedure is performed as described in Section 5.5. And for each calibration instance, we use a different number of trap species ranging from 1 to 5. The obtained results are depicted in Fig. 5.2, which shows the resulting χ^2_r as a function of the number of trap species for a 1D and 2D simulations, for three different damaged profiles (two different signal levels and CI delays). The CDM parameters that realize the best achieved agreement are summarized in Table 5.2.

So far only one detailed study has been dedicated to the characterization of the trap

species present in an irradiated Gaia-like CCD. The results of this study are summarized in Hopkinson et al. (2005). They identified 7 different trap species with release time constants τ ranging from a few μs to several hundred seconds at the Gaia operational temperature. As already discussed, the CTI-induced distortion observed in the damaged charge profile from RC2 is mostly caused by the CTI occurring in the CCD image area. According to the SRH formalism, 67% of the traps release their charge after a time $t = \tau$. Most of the traps with a release time constant significantly shorter than the TDI period (or parallel transfer period), are thus expected to capture and release charges within the time of a single transfer event. As a consequence those traps have no net effect on the stellar image. Considering a Gaia CCD TDI period of 0.9892 ms and looking at Table 1 in Hopkinson et al. (2005), one can infer that 4 out of the 7 identified trap species will contribute to the CTI in the CCD image area. These 4 trap species have the following measured release time constants: 130 s, 2–4 s, 15 ms, and 0.8 ms.
Figure 5.2 clearly shows that 2 trap species are enough to obtain a good agreement between the model and the test data when the CDM parameters are optimized to a fit a single profile. One trap species may also be enough when focusing on shorter CI delays. This is less than the four trap species mentioned above, but this is in agreement with our expectations since an individual profile with a particular CI delay does not set a high constraint on the trap parameters and does not allow an efficient differentiation between trap species with similar effects on the stellar image:

1. The impact on the image profile of traps with a release time constant greater than the CI delay (i.e. $\tau >> t_{\rm CI}$) remains very little.
2. Traps with a release time constant smaller than the CI delay and greater than the temporal size of a window (here $P_{\rm TDI}\times$ 15 pixels) have very similar effects; they are empty prior to the star transit and capture electrons from the profile, but release only very few of them within the window. Two of the trap species mentioned above belong to that interval (for $t_{\rm CI} \sim 27$ s).
3. Traps with short release time constant compared to the window temporal size can capture electrons in the leading edge and release them within the profile, again two of the traps species from Hopkinson et al. (2005) study belong to that interval.

Figure 5.2 also shows that one can obtain the same level of agreement for CDM simulations performed in 1D or 2D. Apart from the necessary additional amount of time to perform one simulation in 2D, it also appears that in the 2D case the CDM calibration generally necessitates a greater amount of simulations to find a similar level of agreement as in the 1D case.
Finally, we investigated the impact of the size of the telemetry window on the best achievable agreement. Fig. 5.1 shows the best agreement obtained for the simulation of a 15 AL pixels window. For stars of magnitude 13.67 and 16.95, the actual telemetry windows for Gaia are composed of respectively 12 and 6 AL pixels. Performing the exact same calibration procedure using the proper size of the telemetry window we obtained a final agreement of $\chi^2_r = 3.78$ for the 13.67 magnitude (12 AL pixels and $t_{\rm CI} \sim 27$ s) and $\chi^2_r = 1.10$ for the 16.95 magnitude (6 AL pixels and $t_{\rm CI} \sim 27$ s). As a

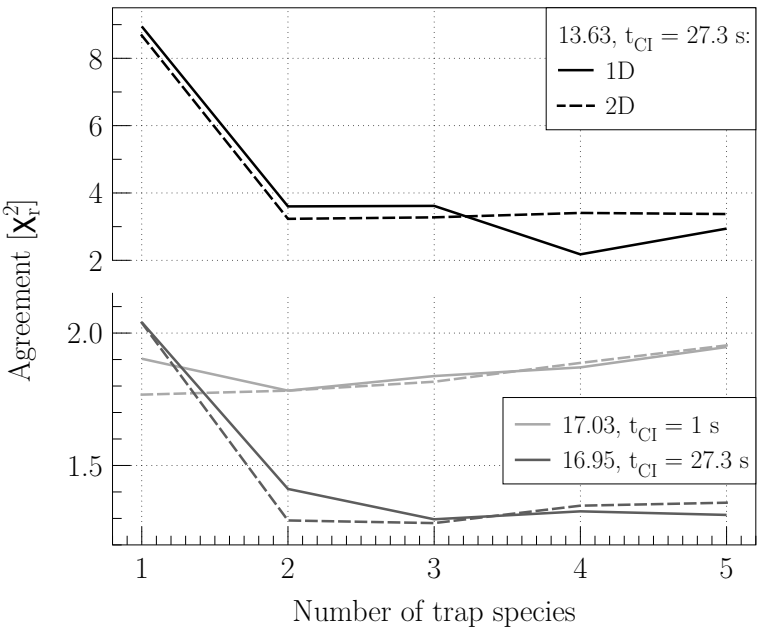

Figure 5.2 — Resulting agreement obtained after a calibration of the CDM parameters for a single charge profile using different number of trap species and performing the CDM simulation in 1 or 2D. The top part of the figure shows the level of agreement as a function of the number of trap species for a target charge profile for G =13.63 and a CI delay of ∼27 s, the bottom part shows the same results for two other target profiles with similar signal levels ($G = 17$) and different CI delays: 1 s (in light grey) and 27 s (in dark grey). The continuous lines depict the results obtained for 1D CDM simulations, and the dashed lines for 2D CDM simulations. While the best agreement possible can be obtained for CDM simulations performed with 2, 3 or 4 trap species depending on the target profile, generally only a minor improvement is achieved by introducing a third or a fourth trap species. Similarly one can notice that the same level of agreement between CDM predictions and test data is obtained for a CDM simulation performed in 1D or in 2D.

consequence the impact of the window size seems to be negligible, however this needs to be further investigated and confirmed.

5.6.2 Calibration on a per magnitude basis

Although a calibration of the CDM parameters performed for a particular damaged profile allow us to investigate the ultimate performance of a CDM candidate, it is unrealistic in the context of the Gaia data processing. We are thus now interested in studying the performance of CDM in more realistic conditions of calibration. In a calibration of the CDM parameter on a per magnitude basis, the resulting set of CDM parameters allows to describe the CTI effects for a particular magnitude (or similar signal levels) and different illumination histories. In this second step we thus fit simultaneously several damaged profiles having similar signal levels but different CI delays. As already mentioned, if a CI fills most of the traps in the CCD only traps with a release time constant similar to or shorter than the CI delay will be empty when the artificial star crosses the CCD. Therefore only these traps cause CTI effects, and with different delays different trap species are important. As a consequence this step also allows us to probe the occurence of trap species with very different release time constants.

Figure 5.3 illustrates the resulting agreement when fitting ten target profiles with G =15 and varying CI delays from 30 ms to 120 s. Fig. 5.3 (left) shows for a particular RC2 profile (G =15 and $t_{\rm CI}$ = 1 s) the difference between the best CDM prediction (see Section 5.6.1) and a CDM prediction based on parameters obtained from the per magnitude calibration. The agreement per profile is very good almost at the level of the best achievable although slightly worse especially in the region of the profile peak as can be seen from the normalized residuals (Fig. 5.3, left bottom). The average χ^2_r achieved for the ten profiles is 8.79.
A careful look at the normalized residuals for each profile that results from a per magnitude calibration (Fig. 5.3, right) shows a subtle systematic variation. It is not clear what causes this systematic variation of the residuals across the image location, yet we can propose some hypotheses. This could be the symptom of an intrinsic limitation of the tested CDM candidate. However such variation seems to be less severe when CDM is fitted to a single profile (Fig. 5.3 left) and absent in most cases (Fig. 5.1) meaning that this limitation is overcome by giving more flexibility to the model. This systematic variation across the image location may originate in the modelling of the CDM input signal (see Section 5.4.3). The construction of the input signal is based on the undamaged reference data accumulated in the non-irradiated part of the CCD. The illumination conditions could have been modified slightly between the acquisition of the CTI-free data and the damaged data. A careful study of the residuals between two CTI-free stellar images located at the top and the bottom of the non-irradiated region of the tested CCD showed that a variation of focus across the CCD produces a similar signature as the one we observed here (C. Crowley (ESA, ESTEC) and Astrium, priv. comm.).
Figure 5.4 shows the variation in mean agreement $\langle\chi^2_r\rangle$ as a function of the number of trap species included in the CDM simulations. As anticipated, to reproduce with a single set of parameters this large dataset that probes different temporal domains, CDM needs several trap species, with different release time constants that cover the CI delay range, and significant densities and cross sections (cf. Table 5.2 column 5). A reasonably good fit can be obtained with 2 or 3 trap species (respectively $\langle\chi^2_r\rangle = 11.39$ and 10.06), however a significant improvement can be obtained by including more trap species. As suggested by the experimental tests (cf. Section 5.6.1 and Hopkinson et al. (2005)), the best agreement is obtained for a number of 4 trap species ($\langle\chi^2_r\rangle = 8.79$). When repeating the exact same calibration procedure for a different magnitude and for the same range of CI delays, we obtain a different set of trap species. As will be further discussed in Section 5.7.1, this can partly be attributed to instabilities in the experimental conditions. Fig. 5.4 also shows that a better agreement can be obtained by performing 1D simulations instead of 2D.

5.6.3 Calibration on a per CCD basis

In this section we are interested in investigating the agreement between experimental data and CDM predictions that results from a calibration of the CDM parameters performed on a per CCD basis. In this case a single set of CDM parameters is used to describe the CTI effects occurring for all the observations acquired with a particular CCD i.e. for any CI delay and at any signal level. This would constitute the least

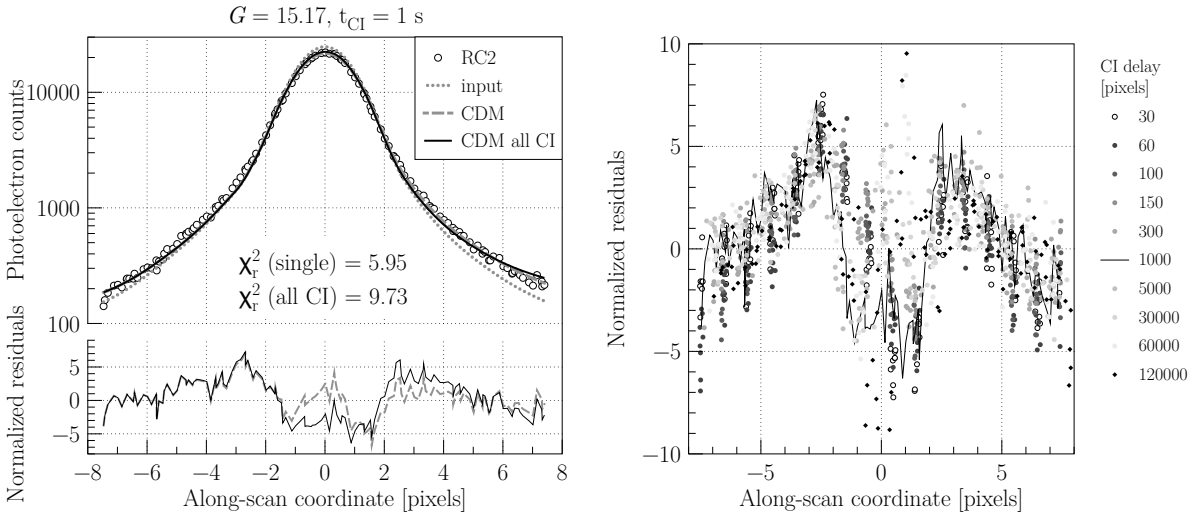

Figure 5.3 — Left: Comparison between the RC2 test data (black circles) and two CDM predictions for the same signal level ($G \sim 15$) and CI delay (~ 1 s). The dashed grey line is a CDM prediction for a parameter set (Table 5.2 column 4) obtained after an individual fit to the depicted RC2 profile, whereas the continuous black line is the CDM prediction for a parameter set (Table 5.2 column 5) obtained after a simultaneous fit to 10 damaged profiles with different CI delays including the one depicted. The dotted grey curve corresponds to the CDM input signal in both cases.
Right: The residuals normalized by the photon noise for each predicted damaged profile resulting from a per magnitude calibration of the CDM parameters.

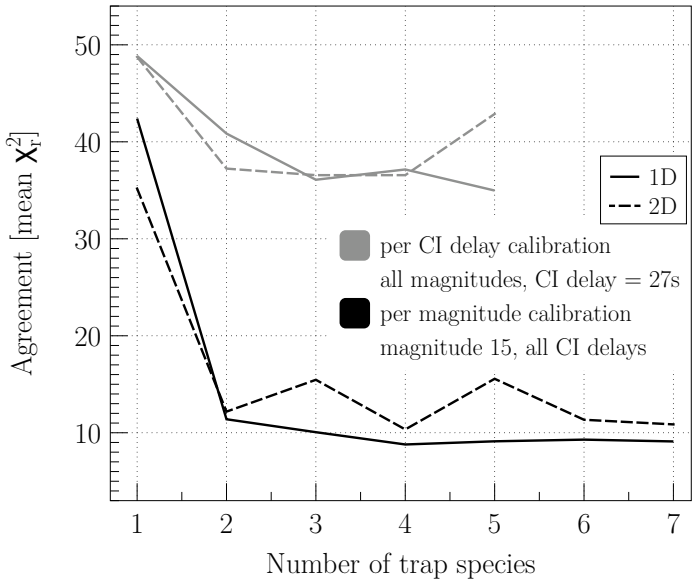

Figure 5.4 — Comparison between the mean agreement obtained after performing a per magnitude (black) and a per CI delay (grey) calibrations of the CDM parameters using different number of trap species and performing the CDM simulation in 1D (continuous line) or 2D (dashed line). In the per magnitude calibration case (black), the test data used to perform the calibration contains 10 damaged over-sampled profiles with $G = 15$ and different CI delays ranging from 30 ms to 120 s. In the per CI delay calibration case (grey), the test data used to perform the calibration contains 5 damaged over-sampled profiles for a CI delay of 27 s and for $G = 13.63, 15.29, 16.95, 18.65, 20.25$.

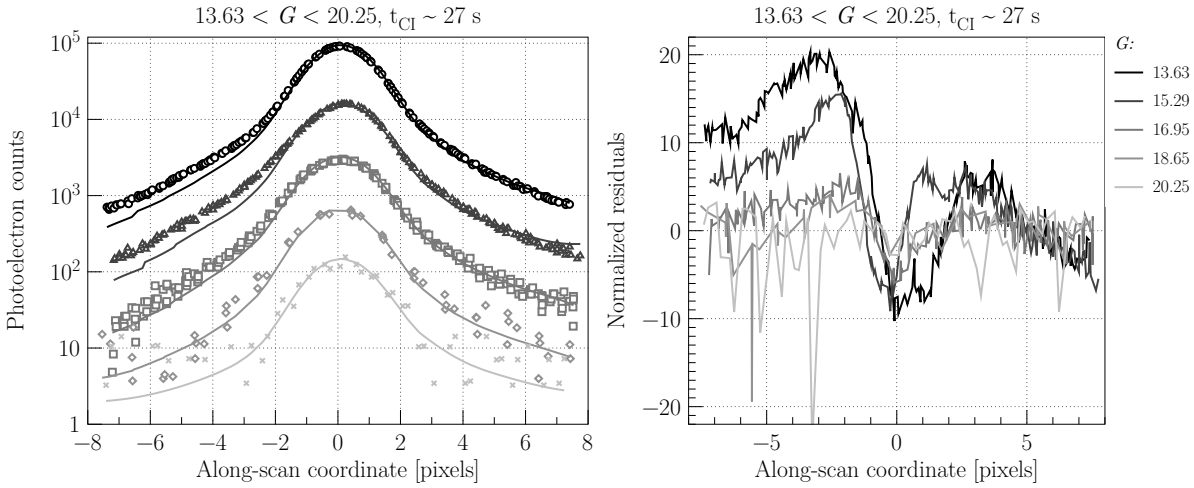

Figure 5.5 — Left: Comparison between the RC2 test data (symbols) and the CDM predictions (continuous lines) for a unique CI delay ($t_{\rm CI} \sim 27$ s) and several signal levels $G = 13.63$, 15.29, 16.95, 18.65, and 20.25. The CDM predictions result from a unique set of parameters (cf. Table 5.2 column 6) obtained by simultaneously fitting the five depicted RC2 damaged profiles.
Right: The residuals normalized by the photon noise for each predicted damaged profile resulting from a per CI delay calibration of the CDM parameters.

cumbersome calibration for the Gaia data processing.

In the previous section we have shown that CDM can fairly well reproduce a set of data including different CI delays at a particular signal level. In a per CCD calibration, CDM will have to deal with different signal levels. Hence we first need to explore how well CDM copes with different brightness levels independently from the illumination history. This is done by fitting with a single set of CDM parameters a set of damaged profiles comprising different magnitudes but similar CI delay. Fig. 5.5 shows a representative example of the level of agreement achieved for such calibration scheme. The overall agreement is clearly poorer than when the fitted dataset contains a unique signal level (Fig. 5.1 and 5.3). A systematic variation of the residuals (Fig. 5.5, right) across the image location similar to the one observed in Fig. 5.3 (right) may be distinguished. But the most prominent residual feature is the strong deviation occurring in the leading edge of the brightest stellar profiles (magnitudes 13.63 and 15.29).

As we shall further explain in Section 5.7.1, it is likely that a single set of trap parameters cannot describe the CTI effects for different signal levels in the context of the RC2 data due to changes in the experimental conditions between tests performed at different magnitudes. However this clear decrease in agreement (see also Fig. 5.4) can partly be imputed to the CDM limitations and in particular to the fact that CDM does not model explicitly the effect of the SBC on the growth of the electron cloud (see Sections 5.2 and 5.3). We indeed observe that reducing the range of signal levels included in our dataset of damaged profiles used in the calibration does improve greatly the resulting mean agreement. For instance, by including only the faintest magnitudes (16.95, 18.65, 20.25) that should experience a similar level of trapping, we obtained a mean agreement of $\langle \chi^2_r \rangle = 3.33$ that should be compared to $\langle \chi^2_r \rangle = 36.08$ when including the whole signal range available in RC2. We thus suggest a modification of CDM so

that the SBC is explicitly taken into account to ease the calibration process. As already discussed by Short et al. (2010), in order to model the effect of a SBC, one may consider to introduce a second parameter β for small charge packets. These two parameters can be constrained by performing experimental measurements on an irradiated CCD such as the fractional charge loss measurement (Chapter 2 and Hopkinson et al. 2005).
Finally we proceed to the calibration of the CDM parameters on a per CCD basis i.e. we perform a simultaneous fit of the CDM predictions to the entire dataset of over-sampled damaged profiles including different CI delays and different signal levels; the resulting χ^2_r for a particular profile is similar to the one resulting from a simultaneous fit to a dataset containing different signal levels only. The highest deviations are systematically obtained for the brightest magnitudes. And again one can obtain a significantly better agreement by removing the brightest damaged stellar images from the fitted dataset. By including only the faintest magnitudes, 16.95, 18.65, 20.25 and CI delays ranging from 30 ms to 30 s, we obtain a very good overall agreement that demonstrates the potential of the tested CDM candidate ($\langle\chi^2_r\rangle = 3.93$) in the context of a per CCD calibration of its parameters.

5.7 Discussion

In this section we interpret the results presented in Section 5.6 and discuss one of the main limits to the agreement between the CDM predictions and the test data: the experimental (Radiation Campaign test setup) instabilities (Section 5.7.1). In the Chapter 3 of this thesis we made use of synthetic data to study the impact of CTI on the image location accuracy. From this study, one can evaluate the level of agreement that any CDM must achieve to recover most of the CTI-induced bias in the image location estimation. Taking into account the experimental instabilities, we discuss the presented CDM performance in the context of these requirements (Section 5.7.2). Finally we discuss and give recommendations regarding the calibration of the CDM parameters during the Gaia mission (Section 5.7.3).

5.7.1 Experimental instabilities

We did not take into account the extra noise contribution induced by experimental instabilities neither in the calibration procedure nor in the comparison criteria, because its accurate measurement is a complicated task. However it is clear from the test data and our results that the experimental instabilities play an important role in limiting the agreement between the CDM predictions and the test data. This is particularly relevant as we aim at reproducing the test data at the noise level (i.e. χ^2_r = 1) and because such instabilities will not be present during the Gaia mission.
One can distinguish between two different types of instability or source of noise. The first is generated by the uncertainty related to the exact knowledge of the experimental conditions: operating temperature, illumination, background level. The CTI effects depend strongly on the temperature, the signal level, and the constant level of illumination or background level. The characteristic release time constant τ varies with the temperature. As a consequence, two tests carried out at different temperatures cannot be explained by CDM with the same value of τ even if the same traps are present in

the CCD. A slight variation in the level of background illumination affects the trap occupancy level prior to the transit of a star: an increase in the background level from 0.3 e^-pixel^{-1} to 5 e^-pixel^{-1} reduces the measured charge-loss from $\sim$ 30% to $\sim$ 10% at magnitude G =18 (Short et al. 2010; Brown 2009a). This variation thus directly affects the calibration of the background light level $S_{\rm DOB}$, and indirectly the trap density parameter for each trap species. To build over-sampled charge profiles we assumed that the experimental conditions remain exactly the same between different scans, i.e. repeated tests. Although this was not generally the case, we did observe in the test data, over-sampled profiles presenting fluctuations with an amplitude greater than the photon noise. Similarly when calibrating the CDM parameters using more than one over-sampled charge profile, we assumed (very) stable experimental conditions between tests carried out for different CI delays or for different signal levels.
The second source relates to the handling of the CCD in between tests carried out during a unique RC. The test data was acquired over a period of several months. A clear variation of the radiation damage effects during the course of a RC has been observed (Georges 2009). In particular, important discrepancies between similar tests carried out at different times have been explained by the fact that during the first three RC the tested CCDs were stored at room temperature in between tests (sometimes up to several days). This seems to affect the trap species characteristics.
Table 5.2 clearly shows that no particular trap species seems to be necessary to explain the data. Although the CDM approximations are not to be forgotten, experimental instabilities certainly play an important role in that matter. As illustrated in Fig. 5.3 (left), the agreement for a particular profile is almost comparable whether the CDM parameters are obtained by fitting a single over-sampled profile or a large set of profiles with the same brightness level (per magnitude calibration). If this noise contribution is one of the main limiting factors to this agreement, we can conclude that the experimental instabilities occurring between two tests with the same brightness and different CI delays have similar amplitudes as instabilities occurring between two scans within the same particular test. As we saw in Section 5.6.3, this agreement for a particular profile can however be considerably deteriorated when including profiles of different brightnesses in the calibration procedure. On top of the limited capabilities of CDM to reproduce CTI effects at different signal levels, this suggests that experimental instabilities between two tests carried out for different signal levels are the largest. This is corroborated by the fact that some of these tests were indeed performed on different days.

5.7.2 The CDM performance in the context of the Gaia approach to CTI mitigation

The Gaia data processing relies on a forward modelling approach to mitigate the CTI effects, in particular to recover the image location bias induced by the stellar image distortion. As a consequence the image location accuracy, and ultimately the Gaia final astrometric accuracy, depends on the capabilities of a CDM to reproduce observations affected by CTI (Chapters 3 and 4). In Section 5.6, we have evaluated the best agreement with the test data achievable by CDM and characterized the variation of this agreement as a function of the applied calibration scheme. Now it is important to evaluate if this agreement is good enough to recover most of the image location bias. To

do so we compare our results to those obtained in Chapter 3 using as test data a large set of synthetic damaged observations generated by a detailed Monte Carlo model of CTI effects (Chapter 2). In this study we applied the Gaia image location estimation procedure on a large set of CTI-free and damaged observations with and without applying the forward modelling CTI mitigation approach. Knowing the exact location of each observation, we are able to measure the residual image location bias after a CTI mitigation using CDM (Fig. 5.6). The original location bias (i.e. without any CTI mitigation) was also measured: for G =15 the bias is of the order of 0.2 pixels and 0.05 pixels for CI delays of respectively 27 and 1 s.

Figure 5.6 shows the agreement between the CDM predictions and synthetic test data as a function of magnitude and for two CI delays (right) and the residual bias when using the same CDM predictions to mitigate the CTI-induced bias (left). There is no clear correlation between agreement and image location bias. This is mainly because our comparison criterion allows a reasonably good agreement to be obtained between

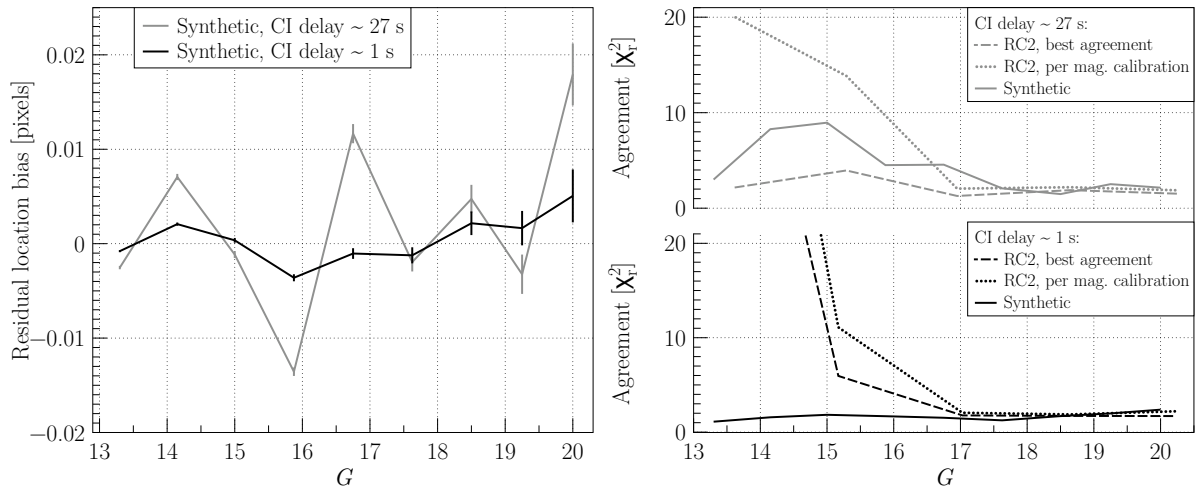

Figure 5.6 — Left: Figure reproduced from Chapter 3. Residual bias in the image location estimation when applying the Gaia image location estimation procedure on synthetic damaged observations including the forward modelling CTI mitigation approach using CDM. The synthetic damaged observations were generated using a detailed and physical Monte Carlo model of CTI effects that simulates the trapping at the trap level, and the charge transfer at the pixel-electrode level (Chapter 2). The residual bias is shown as a function of magnitude and for different levels of active trap densities in the simulated CCD. Active means that these traps are empty prior to the transit of a star. In grey the active trap density is 4 traps pixel^{-1}, in black 1 trap pixel^{-1}. The CTI effects amplitude (charge loss and image location bias) resulting from these particular active trap densities is representative of the CTI effects for a CCD irradiated at the level of 4×10^9 protons cm^{-2} (10 MeV equivalent) but for different CI delay: 27 s (4 traps pixel^{-1}) and 1 s (1 trap pixel^{-1}). To obtain these results the CDM parameters were calibrated to reproduce the damaged observations on a per magnitude basis using one-dimensional CDM simulations, the true instrument LSF was used as an input signal.
Right: Agreement as a function of magnitude between the CDM predictions and the damaged observations: synthetic (continuous line), and RC2 test data (dotted and dashed lines). This agreement is shown for two different CI delays: 1 s (black) and 27 s (grey). In the case of CDM agreement with the RC2 test data, we show the best agreement achieved (dashed line) corresponding to a calibration as described in Section 5.6.1 and the resulting agreement from a calibration on a per magnitude basis (dotted line) as described in Section 5.6.3.

a CDM prediction and a damaged observation, without a perfectly accurate reproduction of the CTI distortion or image shape. Yet the agreement shown guarantees a bias recovery of at least one order of magnitude. However the lack of correlation between the agreement and image location bias is an important indication of the current limits of our comparison criterion which is essentially photometric. We thus recommend the use of a criterion that would properly take into account the profile shape by introducing, for instance, the first derivative of the image profiles.
Figure 5.6 (right) also shows the agreements between the CDM predictions and the RC2 test data obtained for two different calibration schemes: (i) dashed lines, the CDM parameters are calibrated to reproduce a particular profile (Section 5.6.1), it corresponds to the best agreement achievable, (ii) dotted lines, the CDM parameters are calibrated on a per magnitude basis (Section 5.6.2), it corresponds to a realistic calibration scheme in the context of the Gaia data processing. We do not show the agreements resulting from a per CI delay and per CCD calibrations (Section 5.6.3), as the results obtained were not satisfactory. It is clear from Fig. 5.6 (right) that the tested CDM candidate has the capability to reproduce damaged observations at the required level of agreement that would enable a substantial, if not complete, recovery of the image location bias induced by CTI. This is especially true for the fainter magnitudes ($G > 16$) for which the agreement with the RC2 data is comparable to the one obtained with the synthetic data. For these magnitudes the agreement achieved using a realistic calibration scheme is similar to the best agreement possible. Nevertheless at brighter magnitudes, a realistic calibration scheme may not allow to reach a satisfactory agreement especially for a short CI delay (Fig. 5.6 right, bottom). Considering that the experimental noise is not taken into account in our agreement measurement, the results obtained for G =15 may still be acceptable. However for the brightest magnitude of our sample, G =13.6, there is a clear mismatch. This mismatch is present for a short CI delay even for the best agreement achievable. This is unexpected as the agreement obtained in the same calibration conditions and a longer CI delay (27 s) is very good (Fig. 5.6 right, grey dashed line, $\chi^2_r = 2.18$). This mismatch is thus present only when shorter CI delays are introduced in the dataset used in the calibration of the CDM parameters. In order to use the TDI mode only of the tested CDM candidate, we assume that a CI is filling all the traps present in the CCD. The number of traps filled by a CI depends on the CI level. The validity of such approximation breaks down if the CI level is lower than the signal level of interest. In our study, it is the case only for G =13 as for the RC2 data subset used in this study the CI level was 20 000e$^-$. As a consequence it is most likely that our approximation limits the performance of CDM in these particular conditions: short CI delays and signal level higher than the CI level. In any case this issue needs to be investigated further by finding out wether this limitation disappears when initializing the trap occupancy level with the image mode of CDM, prior to a CDM simulation in TDI mode.

5.7.3 Calibrating CDM

On top of its elaboration, the calibration of the chosen CDM is one of the main challenges faced by the Gaia data processing in the context of the CTI mitigation. In this study we have shown that, with the current version of CDM, a set of CDM parameters

per magnitude is necessary to obtain an acceptable reproduction of the damaged observations. In this per magnitude calibration scheme, four trap species must be included in the CDM simulation to obtain satisfactory results. Based on the results obtained for the faintest magnitude only, we also showed that a single set of CDM parameters for all the observations carried out with one CCD is conceivable, provided a modification is made of the way the current CDM is handling the electron cloud growth as a function of signal level.

Nevertheless it is not only the calibration approach that remains to be determined, but also the calibration method itself. Following the overall self calibrating approach chosen for the Gaia data processing, the image parameters, the instrument LSF, and the CDM parameters will be estimated from the same data in an iterative process (Chapter 3 and Prod'homme 2011). This means that such cumbersome calibration procedure as presented in this chapter (evolutionary algorithm probing the whole parameter space and then a fine tuning performed by the simplex downhill method) cannot be used in practice, at least not on a regular basis. It is thus expected that the CDM parameters will be estimated based on a maximum likelihood method, as for the image location estimation procedure. However the very degenerate nature of the CDM parameter space implies that the maximum likelihood method will have to be initialized with parameters already close to optimal. It is presently planned to use as a first guess the information that can be derived from the CI about the trap parameters. The trap density can be inferred from the charge loss occurring in the first pixels of the CI profile. Indications about the cross-section of the traps can be derived from the same measurement. And the characterization of the different trap species, as well as the determination of their release time constant can be achieved by analyzing the release of electrons after a CI. If the CDM parameter search is constrained to realistic values, a CDM candidate capable of very accurately reproducing the damaged observations must do so with a set of physically plausible parameter values.

In that respect the tested CDM candidate performs remarkably well. The interval for each of the free CDM parameters (cf. Table 5.1) was chosen to be physically plausible and also realistic regarding values available in the literature for these parameters. As can be seen from Table 5.2, good agreement with the test data were obtained with values well within those intervals. The diffuse optical background parameter, S_{DOB}, is generally found to be close to the one measured directly from the RC2 test data. Regarding the values of the β parameter, they were systematically found within the range [0, 0.3] this is in agreement with what is expected for a Gaia CCD (cf. Short et al. 2010). Nevertheless it is surprising that in some cases a better level of agreement can be obtained by performing one- rather than two-dimensional CDM simulations, since the CTI effects varies with the signal level and that the signal level vairation over a stellar profile in the AC direction is important. This may be partly attributed to the necessary assumptions required to build a two-dimensional input signal (Section 5.4.3). However similar levels of agreement for 1D or 2D CDM simulations were also found when using synthetic test data where there is no ambiguity regarding the input signal (Chapter 3). A more realistic modelling of the electron cloud growth with the signal level using two different values for β may also improve the results obtained for 2D simulations.

5.8 Conclusions and future work

The final astrometric accuracy of Gaia is conditioned on the capability of a CDM to reproduce observations affected by CTI. Using a detailed and rigorous comparison procedure, we established the current level of performance of the tested CDM candidate to reproduce experimental test data representative of the future Gaia observations. We showed that at low signal levels ($G > 15$) CDM is capable of reproducing damaged profiles accurately enough to enable a factor of ten recovery of the image location bias induced by CTI during the Gaia mission, provided that the CDM parameter calibration follows a certain scheme.

When the CDM parameters are calibrated to reproduce a single profile for a particular CI delay and signal level, the agreement between the CDM prediction and this profile is remarkable and this for the whole range of tested magnitudes ($13 < G < 20$) and CI delays (from 30 ms to 120 s). The worst agreement was obtained for the brightest magnitude and shortest CI delay. This may be explained by our assumption that a CI fills all the traps present in the CCD independently from its level. Such assumption can be avoided by a proper treatment of the effect of CIs on the trap occupancy level prior to the a stellar transit.

With a single set of parameters, CDM is capable of reproducing up to a certain level a set of experimental data including different CI delays and magnitudes. In the context of Gaia and considering a realistic calibration scheme, this level of agreement is only acceptable when the CDM parameters are calibrated on a per magnitude basis, that is to say if a different set of CDM parameters is used for each magnitude. In these calibration conditions, a CDM simulation can be performed in one or two dimensions and must include at least four different trap species.

Due to its way of handling the growth of the electron cloud as a function of signal level with a single parameter β, CDM is currently not able to reproduce the effect of the supplementary buried channel. This constitutes one of the main limitations of the current CDM when it is used to reproduce with a single set of parameters a set of experimental data that involves different brightness levels. It has to be noted that, in these calibration conditions, the instabilities in the experimental conditions also played an important role in limiting the best agreement achievable.

The CDM performance appears to be acceptable if the set of data that CDM aims to reproduce contains only signal levels for which the effect of the SBC is similar. This suggests that a calibration of the CDM parameters for signals levels of similar brightness on a per CCD basis remain a viable option for the Gaia data processing consortium.

The tested CDM can achieve the required level of agreement by using physical and realistic trap parameters. Hence we are confident that the CDM parameter calibration will be eased and benefit from a determination of the trap parameters using the CI onboard Gaia. However this remains to be studied in more detail, in particular by using the imaging mode of CDM to reproduce CIs and check that the trap parameters obtained are similar to the ones directly inferred from the CI. Currently the effects of the serial CTI on the image location estimation procedure and the CTI mitigation scheme remains unclear. The native serial CTI is expected to be the predominant source of image distortion at the beginning of the mission, when the CTI induced by radiation

damage is still mild. It is thus also important to evaluate the performance of CDM to reproduce stellar images affected by both serial and parallel CTI. Finally, in order to improve the image location bias recovery, we plan to investigate the use of a new comparison criterion in the CDM calibration procedure that would quantify not only the reproduction of the image flux but also of the image shape.

Acknowledgments

The authors would like to acknowledge EADS Astrium for kindly supplying the experimental test data necessary to accomplish the presented study and the participants of the Gaia Radiation Task Force for providing useful feedback. The work of TP and MW was funded by the European Community's sixth framework programme (FP6) through the Marie Curie research training network ELSA (European Leadership in Space Astrometry, MRTN-CT-2006-033481). AB acknowledges support by the Netherlands Research School for Astronomy (NOVA).

Calibration	per over-sampled profile				per magnitude	per CI delay
Section	5.6.1				5.6.2	5.6.3
Figure	5.1	5.1	-	5.3 (left)	5.3	5.5
Target data:						
Magnitude	13.67	16.96	17.03	15.17	~ 15	13 to 20
CI delay	27 s	27 s	1 s	1 s	30 ms to 120 s	27 s
Agreement $[\chi^2_r]$	2.18	1.28	1.77	5.95	8.79*	36.08*
CDM parameters:						
Simulation	1D	2D	2D	1D	1D	1D
β	0.21	0.28	0.23	0.36	0.15	$6.49\ 10^{-2}$
dob [$e^- s^{-1}$ sample^{-1}]	3.31	$9.28\ 10^{-4}$	46.53	240.0	24.54	1.43
ρ_1 [per sample]	2.37	9.09	21.87	2.35	4.35	5.33
σ_1 [m^2]	$1.48\ 10^{-23}$	$4.08\ 10^{-23}$	$4.67\ 10^{-22}$	$1.00\ 10^{-23}$	$4.71\ 10^{-23}$	$1.44\ 10^{-22}$
τ_1 [s]	$2.06\ 10^{-3}$	$4.47\ 10^{-3}$	$1.01\ 10^{-1}$	$2.58\ 10^{-3}$	$6.43\ 10^{-2}$	$9.64\ 10^{-2}$
ρ_2	7.52	$1.86\ 10^{-2}$	-	20.0	17.86	$7.37\ 10^{-2}$
σ_2	$1.23\ 10^{-23}$	$5.72\ 10^{-18}$	-	$3.69\ 10^{-23}$	$1.00\ 10^{-23}$	$1.73\ 10^{-18}$
τ_2	2.37	$3.09\ 10^{-1}$	-	0.60	0.91	$2.53\ 10^{-1}$
ρ_3	4.51	5.65	-	-	5.47	4.72
σ_3	$4.21\ 10^{-22}$	$9.40\ 10^{-22}$	-	-	$3.60\ 10^{-22}$	$2.42\ 10^{-18}$
τ_3	39.86	2.84	-	-	7.59	20.55
ρ_4	3.55	-	-	-	17.67	-
σ_4	$9.93\ 10^{-20}$	-	-	-	$9.28\ 10^{-22}$	-
τ_4	42.06	-	-	-	99.92	-

Table 5.2 — The different sets of CDM parameters that achieved the best agreement for the different calibration schemes presented.
* this value corresponds to the mean agreement $\langle \chi^2_r \rangle$ considering all the profiles used in this particular calibration scheme.